Pergamon

Int. J. Heat Mass Transfer. Vol. 37, No. 11, pp. 1619–1630, 1994

0017-9310/94 $7.00+0.00

0017-9310(94)E0011-I

A finite difference calculation of forced convective heat transfer from an oscillating cylinder

D. KARANTH, G. W. RANKIN† and K. SRIDHAR

Department of Mechanical Engineering and Fluid Dynamics Research Institute, University of Windsor, Windsor, Ontario, Canada, N9B 3P4

(*Received* 19 *February* 1993 *and in final form* 6 *December* 1993)

Abstract—A finite difference calculation of forced convective heat transfer from an oscillating cylinder is carried out using vorticity, stream function and temperature as the dependent variables. The non-dimensionalized vorticity transport and energy equations in a non-inertial frame attached to the cylinder, are solved in a rectangular grid, based on a log–polar coordinate system. The effects of cylinder oscillation in the in-line and transverse directions, on the time dependent average Nusselt number and the Nusselt number distribution on the cylinder surface are investigated for a Reynolds number of 200. Some of the numerical predictions are compared with experimental data available in the literature. In the case of the stationary cylinder, the average Nusselt number was found to oscillate at twice the natural shedding frequency. The heat transfer rate from the oscillating cylinder increases with the increasing velocity amplitude. In the case of transverse oscillation, the location of maximum local Nusselt number was found to oscillate between the upper and lower surface of the cylinder. Contour maps of vorticity, stream line and isotherms are presented and the physical aspects of the flow field are discussed.

INTRODUCTION

THE FORCED convective heat transfer from a stationary cylinder is a fundamental engineering problem with applications ranging from heat exchangers to hot wire anemometers. Experimental observations and numerical predictions have shown that the alternating vortex street in the wake of a cylindrical body induces oscillating lift and drag forces on the body. The unsteady behaviour of the flow close to the surface strongly affects the heat transfer from the cylinder. The oscillating lift and drag forces may cause the cylindrical body to vibrate both in the in-line and transverse directions. In order to design the heating elements to withstand the vibration or to improve the heat transfer rate, it is necessary to investigate the effects of oscillation of the cylinder in the in-line and transverse directions.

In the past two decades, several numerical investigations of the unsteady heat transfer from a stationary circular cylinder have been made. Most of these were carried out for Reynolds number less than 500. Recently, Chun and Boehm [1] carried out a finite difference calculation of forced convective heat transfer at various Reynolds numbers as high as 3480 without initiating an alternating vortex street. Many experimental correlations exist relating the Reynolds number, Prandtl number and the mean Nusselt number for the case of forced convective heat transfer from a stationary cylinder.

Many experimental investigations have shown that oscillation of the cylinder in a still fluid medium results in an increased heat transfer rate [2–5]. In the case of an oscillating cylinder in a cross flow, fewer experimental studies have been reported in the literature. Hegge Zijnen [6] observed a decrease in the heat transfer rate at a Reynolds number of 5 with the cylinder undergoing oscillation in the direction in-line to that of the mean flow. Leung *et al.* [7] observed an enhanced heat transfer rate for Reynolds numbers less than about 15 000 with in-line oscillation. At Reynolds numbers 1400, 2100 and 3500, Takahashi and Endoh [8] experimentally investigated the effects of in-line oscillation of the cylinder on the heat transfer rate at various vibrational Reynolds numbers and concluded that heat transfer rate increased during the in-line oscillation above certain velocity amplitude. Sreenivasan and Ramachandran [9] experimentally studied the effects of the oscillation of a cylinder in the direction transverse to that of the air stream and no appreciable change in the heat transfer coefficient was observed with a maximum velocity amplitude of 0.2. At a Reynolds number of 3500, Saxena and Laird [10] observed that some local heat transfer coefficients were up to 60% larger with a vertical cylinder undergoing forced oscillations in the direction transverse to the mean

† To whom correspondence should be addressed.

NOMENCLATURE

a	transformation parameter
A'_x, A'_y	velocity amplitude in the in-line and transverse direction respectively [m s^{-1}]
A_x, A_y	nondimensional velocity amplitude in the in-line and transverse direction respectively
R	radius of the cylinder [m]
F_x, F_y	nondimensional frequency parameter in the in-line and transverse direction, respectively
$Nu(\theta, \tau)$	local Nusselt number (as defined in equation (14))
$Nu_{avg}(\tau)$	average Nusselt number (as defined in equation (15))
Nu_m	mean Nusselt number (as defined in equation (16))
Pr	Prandtl number
(r, θ)	radial and tangential coordinates in a frame of reference attached to the cylinder
Re	Reynolds number
T	temperature [°C]
T_s	cylinder surface temperature [°C]
T_∞	ambient temperature [°C]
t	time [s]
t_x, t_y	period of oscillation in the in-line and transverse direction respectively [s]
U, V	nondimensional convective velocity component in the ξ and η direction, respectively
U'	free stream velocity [m s^{-1}]
U^*	nondimensional free stream velocity relative to the frame of reference attached to the cylinder
v_r, v_θ	relative velocity component in the r and θ direction respectively [m s^{-1}]
V_r, V_θ	nondimensional relative velocity component in the r and θ direction, respectively
(x, y)	Cartesian coordinates in the frame of reference attached to the cylinder
(x', y')	Cartesian coordinates in the inertial frame of reference
x'_c, y'_c	position of the cylinder in the in-line and transverse direction respectively [m].

Greek symbols

α	thermal diffusivity [m^2 s^{-1}]
ε	incident angle of the nondimensional free stream velocity relative to the frame of reference attached to the cylinder
ν	kinematic viscosity [m^2 s^{-1}]
(ξ, η)	nondimensional log–polar coordinates
τ	nondimensional time
τ_{cycle}	nondimensional time in a natural vortex shedding cycle or an oscillation cycle of the cylinder
τ_n	nondimensional natural vortex shedding period
τ^*	ratio, τ_{cycle}/τ_n
Φ	nondimensional temperature
ψ	stream function relative to the frame of reference attached to the cylinder [m^2 s^{-1}]
Ψ	nondimensional stream function relative to the frame of reference attached to the cylinder
ω	vorticity [s^{-1}]
Ω	nondimensional vorticity.

water flow. Other investigators such as Kezios and Prasanna [11] reported a 20% increase in the average heat transfer coefficient with a transversely oscillating cylinder. In the literature, no conclusive experimental results have been reported regarding the effects that an oscillating cylinder has on the forced convective heat transfer.

Flow past an oscillating cylinder either in the in-line or transverse direction has been experimentally and numerically studied by several researchers for many years. Several finite difference or finite volume simulations [12–15] have been carried out using the concept of a non-inertial frame of reference. All of the simulations were carried out using the primitive variables except for Lecointe [15]. To the authors' knowledge, no numerical simulation has been attempted to study the effects of oscillation of the cylinder on forced convective heat transfer.

In the case of flow past a stationary cylinder, vortices are shed at a constant nondimensional natural shedding frequency (Strouhal number), for a flow with a particular Reynolds number. Within a range of forced frequency, vortex shedding is controlled by the oscillation of the cylinder and a considerable increase in the lift and drag force is observed. This is referred to as the 'lock-in', 'wake capture' or 'synchronization' phenomenon. During transverse oscillation, lock-in occurs when the forced frequency approaches the natural shedding frequency causing a considerable increase in the drag force with the vor-

tices being shed at the same frequency as that of the cylinder. The lock-in phenomenon occurs with an in-line oscillation, when the frequency of the cylinder approaches twice the natural shedding frequency. The vibration of the cylinder in the lock-in range of frequencies, causes the vortex shedding to occur at half the cylinder frequency and produces a significant increase in the lift force. The influence of the lock-in phenomenon on the heat transfer is rarely discussed in the literature.

The main objective of this paper is to study the effects that oscillation of the cylinder in the in-line and transverse directions has on the time history of the average Nusselt number over the cylinder surface. It is also of importance to bring out the influence of cylinder oscillation on the local Nusselt number distribution on the surface of the cylinder. The effect that the lock-in phenomenon has on the heat transfer rate is also discussed. The influence of alternating vortex street on the isotherm contours and the time history of the Nusselt number is also examined.

In this study, the non-dimensionalized vorticity transport and energy equations in a non-inertial reference frame (attached to the cylinder) are solved on a rectangular grid based on log–polar coordinates (ξ, η). Finite difference calculations were made at a Reynolds number of 200. Laminar flow assumption is made and the Prandtl number is assumed to be 1.0.

FORMULATION

The isothermal cylinder is assumed to be oscillating sinusoidally either in the in-line or transverse direction to that of the mean flow (Fig. 1). In order to achieve a fixed grid with respect to the cylinder, it is necessary to use a non-inertial reference frame attached to the cylinder $(x, y$ or $r, \theta)$. The governing equations in the case of a two dimensional flow problem are the continuity, energy and two momentum component equations. By introducing the stream function and vorticity into the continuity and momentum equations, they can be simplified and reduced to two equations: the vorticity transport equations. In the case of an oscillating cylinder, the vorticity transport equations and the energy equation in a non-inertial reference frame retain the same form as in the inertial frame of reference and are given by

$$\frac{\partial \omega}{\partial t} + \frac{1}{r}\left[\frac{\partial}{\partial r}\left(\omega \frac{\partial \psi}{\partial \theta}\right) - \frac{\partial}{\partial \theta}\left(\omega \frac{\partial \psi}{\partial r}\right)\right] = \nu \nabla^2 \omega \quad (1)$$

$$\omega = -\nabla^2 \psi. \quad (2)$$

$$\frac{\partial T}{\partial t} + \frac{1}{r}\left[\frac{\partial}{\partial r}\left(T \frac{\partial \psi}{\partial \theta}\right) - \frac{\partial}{\partial \theta}\left(T \frac{\partial \psi}{\partial r}\right)\right] = \alpha \nabla^2 T \quad (3)$$

where

$$\nabla^2 = \frac{\partial^2}{\partial r^2} + \frac{1}{r}\frac{\partial}{\partial r} + \frac{1}{r^2}\frac{\partial^2}{\partial \theta^2}.$$

The relative velocity components in the radial and tangential directions are defined as follows

$$v_r = \frac{1}{r}\frac{\partial \psi}{\partial \theta}, \quad v_\theta = -\frac{\partial \psi}{\partial r}. \quad (4)$$

In order to achieve a more accurate numerical solution, it is essential to have a finer grid near the cylinder. This can be accomplished by the use of the log–polar co-ordinate transformation given by:

$$r/R = e^{a\xi} \quad \text{and} \quad \theta = a\eta$$

where 'a' the transformation parameter is set equal to π in this study.

This log–polar co-ordinate transformation allows us to have a uniform grid in a transformed rectangular domain. The nondimensional variables are defined as:

$$\tau = \frac{tU'}{R}, \quad \Psi = \frac{\psi}{RU'}, \quad \Omega = \frac{\omega R}{U'}, \quad \Phi = \frac{T - T_\infty}{T_s - T_\infty},$$

$$V_r = \frac{v_r}{U'}, \quad V_\theta = \frac{v_\theta}{U'}, \quad Re = \frac{2RU'}{\nu}, \quad Pr = \frac{\nu}{\alpha},$$

$$A_x = \frac{A'_x}{U'}, \quad A_y = \frac{A'_y}{U'}, \quad F_x = \frac{2R}{t_x U'}, \quad F_y = \frac{2R}{t_y U'}.$$

The nondimensionalized vorticity transport and energy equations are

$$g(\xi)\frac{\partial \Omega}{\partial \tau} + \frac{\partial}{\partial \xi}\left(\Omega \frac{\partial \Psi}{\partial \eta}\right) - \frac{\partial}{\partial \eta}\left(\Omega \frac{\partial \Psi}{\partial \xi}\right) = \frac{2}{Re}\nabla^2 \Omega \quad (5)$$

$$g(\xi)\Omega = -\nabla^2 \Psi \quad (6)$$

$$g(\xi)\frac{\partial \Phi}{\partial \tau} + \frac{\partial}{\partial \xi}\left(\Phi \frac{\partial \Psi}{\partial \eta}\right) - \frac{\partial}{\partial \eta}\left(\Phi \frac{\partial \Psi}{\partial \xi}\right) = \frac{2}{Re\,Pr}\nabla^2 \Phi \quad (7)$$

where

$$g(\xi) = a^2 e^{2a\xi}$$

and

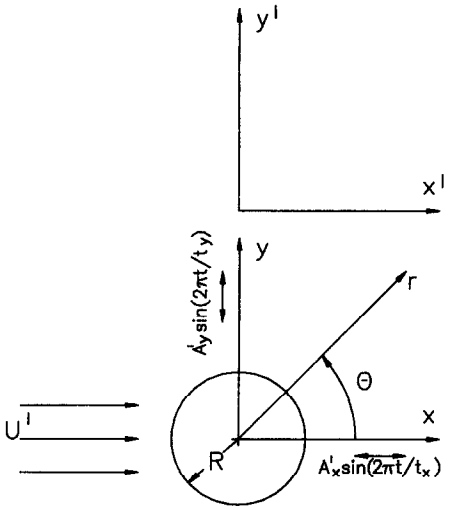

FIG. 1. Coordinate systems.

$$\nabla^2 = \frac{\partial^2}{\partial \xi^2} + \frac{\partial^2}{\partial \eta^2}.$$

The nondimensional relative velocity components are given by

$$V_r = \frac{U}{\sqrt{(g(\xi))}}, \quad V_\theta = \frac{V}{\sqrt{(g(\xi))}} \tag{8}$$

where

$$U = \frac{\partial \Psi}{\partial \eta}, \quad V = -\frac{\partial \Psi}{\partial \xi}.$$

The boundary conditions on the cylinder surface are given by

$$\Psi = \frac{\partial \Psi}{\partial \xi} = 0, \quad \Omega = -\frac{1}{a^2}\left(\frac{\partial^2 \Psi}{\partial \xi^2}\right)_0, \quad \Phi = 1 \text{ on } \xi = 0.$$

The time dependent far field boundary condition for the stream function relative to the cylinder is obtained by using the potential flow solution.

$$\Psi = 2[(1 - A_x \sin(\pi \tau F_x))^2 + (A_y \sin(\pi \tau F_y))^2]^{1/2} \times \sinh(a\xi_\infty) \sin(a\eta - \varepsilon)$$

where

$$\varepsilon = \tan^{-1}\left[\frac{-A_y \sin(\pi \tau F_y)}{1 - A_x \sin(\pi \tau F_x)}\right].$$

The nondimensionalized temperature and vorticity in the far field are assumed to be zero. Based on the information available in the literature, the far field boundary may be located at a distance of 80 times the cylinder radius.

NUMERICAL PROCEDURE

The vorticity transport and the energy equations are solved numerically using the ADI scheme. Borthwick [16] showed that the ADI scheme is more reliable and accurate than the upwind directional difference explicit scheme. The time derivative is approximated using forward difference and the diffusion and convective terms are calculated using the central difference scheme. The vorticity transport equation in a two step finite difference form is given as follows.

$$\frac{2g(\xi_j)}{\Delta \tau}\Omega_{i,j}^{n+1/2} + \left(\frac{(V^n\Omega^{n+1/2})_{i+1,j} - (V^n\Omega^{n+1/2})_{i-1,j}}{2\Delta\eta}\right) - \frac{2}{Re}\left(\frac{(\Omega_{i+1,j} - 2\Omega_{i,j} + \Omega_{i-1,j})^{n+1/2}}{\Delta\eta^2}\right) = \frac{2g(\xi_j)}{\Delta \tau}\Omega_{i,j}^{n} - \left(\frac{(U\Omega)_{i,j+1}^n - (U\Omega)_{i,j-1}^n}{2\Delta\xi}\right) + \frac{2}{Re}\left(\frac{(\Omega_{i,j+1} - 2\Omega_{i,j} + \Omega_{i,j-1})^n}{\Delta\xi^2}\right) \tag{9}$$

$$\frac{2g(\xi_j)}{\Delta \tau}\Omega_{i,j}^{n+1} + \left(\frac{(U^n\Omega^{n+1})_{i,j+1} - (U^n\Omega^{n+1})_{i,j-1}}{2\Delta\xi}\right) - \frac{2}{Re}\left(\frac{(\Omega_{i,j+1} - 2\Omega_{i,j} + \Omega_{i,j-1})^{n+1}}{\Delta\xi^2}\right) = \frac{2g(\xi_j)}{\Delta \tau}\Omega_{i,j}^{n+1/2} - \left(\frac{(V^n\Omega^{n+1/2})_{i+1,j} - (V^n\Omega^{n+1/2})_{i-1,j}}{2\Delta\eta}\right) + \frac{2}{Re}\left(\frac{(\Omega_{i+1,j} - 2\Omega_{i,j} + \Omega_{i-1,j})^{n+1/2}}{\Delta\eta^2}\right). \tag{10}$$

The superscript n represents the nth time step and the subscripts i,j represent the (i,j) mesh point in the (η, ξ) coordinates, respectively. Similarly, the energy equation can be written in the finite difference form by replacing the dependent variable with Φ and the Reynolds number with the product of Reynolds number and Prandtl number.

The velocities in the convective terms are calculated using the fourth order accurate Hermitian relations and are given by

$$U_{i-1,j} + 4U_{i,j} + U_{i+1,j} = \frac{3}{\Delta\eta}(\Psi_{i+1,j} - \Psi_{i-1,j}) \tag{11}$$

$$V_{i,j-1} + 4V_{i,j} + V_{i,j+1} = \frac{-3}{\Delta\xi}(\Psi_{i,j+1} - \Psi_{i,j-1}). \tag{12}$$

The Hermitian relations have been used successfully by Loc and Bouard [17] up to a Reynolds number of 9500. The vorticity boundary condition on the cylinder can be approximated numerically in different ways. In this study, a second order accurate cubic polynomial approximation is used and is given by

$$\Omega_{i,0} = -\frac{1}{a^2}\left(\frac{8\Psi_{i,1} - \Psi_{i,2}}{2\Delta\xi^2}\right). \tag{13}$$

The Poisson equation is solved iteratively using the SOR scheme. An optimum relaxation coefficient [18] is used to enhance the convergence rate. The numerical solution obtained is first order accurate in time and second order accurate in space. The grid dependency tests were carried out using 121×85, 151×106 and 181×127 grid sizes for the case of stationary cylinder. The 151×106 and 181×127 grids gave similar results. In this study, the nondimensional time step and the grid size are taken to be 0.01 and 151×106, respectively. The far field boundary was located at distance of $81.3R$ ($\xi_{max} = 1.4$). In the initial stage of simulation, the cylinder was rotated counterclockwise and then clockwise for a small duration of time with a constant angular velocity. This numerical triggering procedure is required to initiate the alternating vortex street [19].

RESULTS AND DISCUSSIONS

The heat transfer between the cylinder and the surrounding stream of fluid is calculated in the form of a

nondimensional number, the Nusselt number. The local Nusselt number is calculated using the following equation

$$Nu(\theta,\tau)=\frac{-2}{a}\left(\frac{\partial\Phi}{\partial\xi}\right)_{\xi=0}. \quad (14)$$

The average Nusselt number represents the net heat transfer from the cylinder surface to the fluid and is expressed as follows

$$Nu_{\text{avg}}(\tau)=\frac{1}{2\pi}\int_0^{2\pi} Nu(\theta)\,\mathrm{d}\theta. \quad (15)$$

In order to compare with the experimental results, it is essential to calculate the mean Nusselt number over a period of time. In this study, mean Nusselt number was calculated between $\tau = 40$ and 100 using the following expression.

$$Nu_{\text{m}}=\frac{1}{60}\int_{40}^{100} Nu_{\text{avg}}(\tau)\,\mathrm{d}\tau. \quad (16)$$

The numerical predictions are compared with the following experimental correlation deducd from refs. [6, 20]

$$Nu_{\text{m}}=0.42+0.57(1-\tfrac{1}{16}A_x^2+\tfrac{1}{8}A_y^2)\sqrt{(Re)}. \quad (17)$$

Stationary cylinder in a cross flow

Figure 2 shows the time dependent average Nusselt number ($Nu_{\text{avg}}(\tau)$). After a stable alternating vortex street is generated in the wake ($\tau \approx 20.0$), the $Nu_{\text{avg}}(\tau)$ was found to be oscillating at twice the natural shedding frequency about a mean value of 8.47. This may be explained by the shedding of two vortices (one from the upper and the other from the lower half of the cylinder) in a complete vortex shedding cycle. The

Table 1. Mean Nusselt number at different velocity amplitudes

A_x	A_y	Computed Nu_{m}	Equation (17) Nu_{m}
0	0	8.470	8.481
0.25	0	8.640	8.450
0.5	0	8.974	8.355
0	0.25	8.588	8.544
0	0.5	8.861	8.733

predicted mean Nusselt number (Table 1) is approximately equal to the value given by the correlation of Kramer [20]. The amplitude of oscillation of the $Nu_{\text{avg}}(\tau)$ was very small (≈ 0.045) when compared to the mean value. The non-dimensional natural shedding frequency was calculated to be equal to 0.2 which agrees exactly with the computed value by Lecointe and Piquet [15]. The corresponding non-dimensional natural vortex shedding period (τ_{n}) is 10. Figure 3 shows the local Nusselt number distribution on the cylinder at different τ^* in a complete vortex shedding cycle. It can be observed that the local Nusselt number distribution does vary only on the down stream side of the cylinder where the vortices are shed alternately. The maximum heat transfer rate occurs at the upstream stagnation point and the minimum heat transfer occurs between the separation points and downstream stagnation point ($\theta \approx 53$ and 308°). Figures 4(a), (b) and (c) show the contour maps of streamline, vorticity and isotherms, respectively, at the same instant of time. The stream line contour map clearly depicts the alternating vortex street in the wake and a vortex being shed from the top half of the cylinder. As both vorticity and thermal energy are being transported by the flow in the wake, the contour maps of vorticity and isotherms have some similar

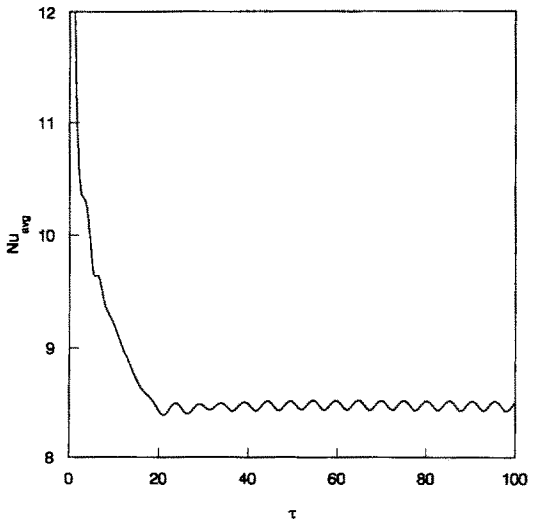

FIG. 2. Time dependent average Nusselt number (stationary cylinder).

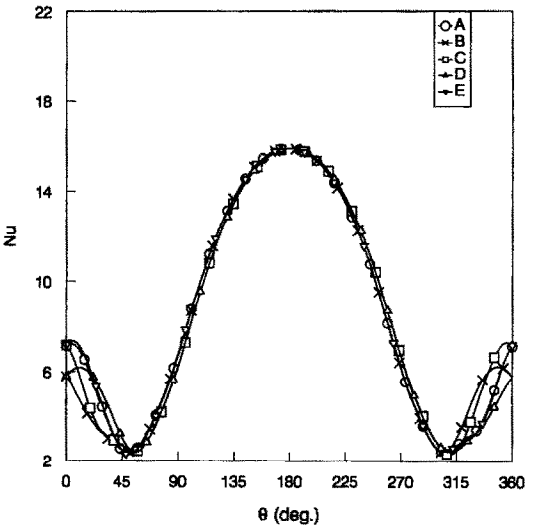

FIG. 3. Local Nusselt number distribution on the cylinder (stationary cylinder). A. $\tau^* = 0.0$, B. $\tau^* = 0.25$, C. $\tau^* = 0.5$, D. $\tau^* = 0.75$, E. $\tau^* = 1.0$.

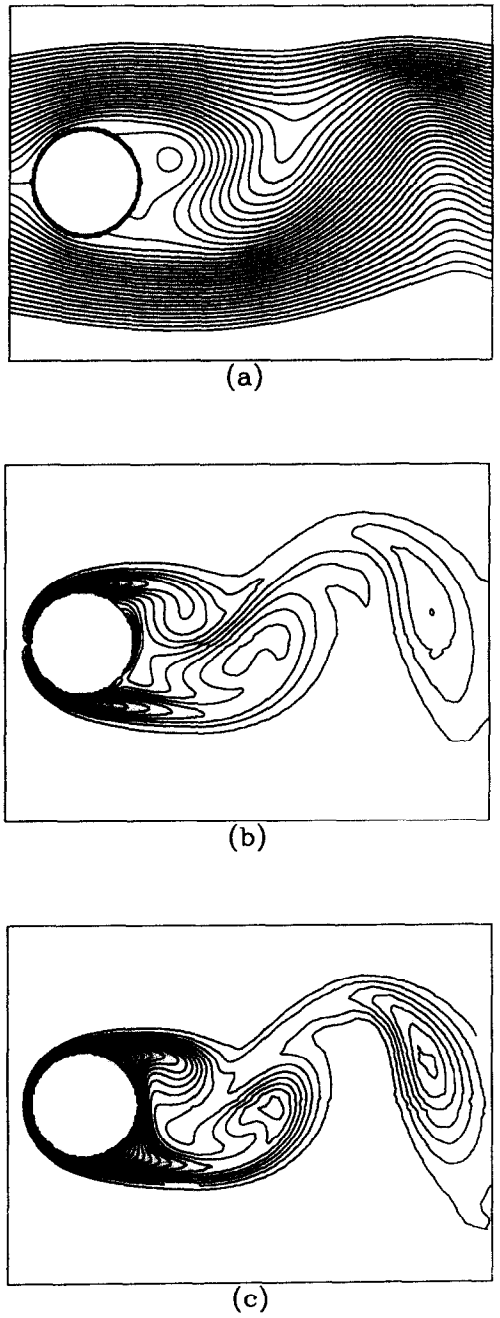

FIG. 4. Contour maps at $\tau = 50.0$ (stationary cylinder). (a) Streamline; (b) vorticity; (c) isotherms.

features. All the isothermal contour maps presented in this paper are with a contour interval of 0.05 and with the minimum and maximum levels of contour as 0.05 and 1.0, respectively.

In-line oscillation

The cylinder was forced to oscillate with a frequency parameter (F_x) of 0.2 and with velocity amplitudes (A_x) of 0.25 and 0.5. The equivalent position amplitudes are $0.4R$ and $0.8R$, respectively. The oscillation of the cylinder was started after a non-dimensional time delay of 40.0. The selected frequency parameter is one-half of the non-dimensional lock-in frequency. Figure 5 shows the time histories of $Nu_{avg}(\tau)$ with $A_x = 0$, 0.25 and 0.5, respectively. The time variation of the position of the cylinder (x_c'/R) and relative free stream velocity ($U^* = 1 - A_x \sin(\pi F_x \tau)$) are also shown in the same figure for reference. The amplitude of $Nu_{avg}(\tau)$ and the mean Nusselt number (Nu_m) increase with the increasing A_x (Table 1). According to equation (17), Nu_m should decrease with the increasing velocity amplitude. Hegge Zijnen [6] verified the equation (17) only up to a Reynolds number of 5. The computed trend of increasing heat transfer rate with the velocity amplitude agrees with the experimental results given by Takahashi and Endoh [8] at higher Reynolds numbers. The average Nusselt number reaches a maximum and a minimum value in a full cycle of forced oscillation. These maximum and minimum values, however, change from cycle to cycle. The maximum values of $Nu_{avg}(\tau)$ in all oscillation cycles are attained when the cylinder moves in the opposite direction to that of the flow and near the zero position of the cylinder ($x_c'/R \approx 0.0$). The minimum values are reached with the cylinder moving in the same direction as that of the flow and near the maximum x_c'/R.

Figures 6(a) and (b) show the local Nusselt number distribution on the cylinder at different times in a full cycle of oscillation (from $\tau = 50.0$ to 60.0) at velocity amplitudes 0.25 and 0.5, respectively. The location and magnitudes of the maximum heat transfer rate at different instants of time during one complete cycle of oscillation are listed in Table 2. On the upstream side of the cylinder, the Nusselt number distribution almost repeats itself after a complete cycle of oscillation. With the velocity amplitude of 0.5, the maximum heat transfer rate occurs near the downstream stagnation point when the cylinder is moving in the same direction as that of the flow. This may be due to the cylinder traversing with significant velocity through the wake which may cause high temperature gradients near the down stream stagnation point. Figures 7(a)–(e) show the contour maps of the isotherms at different stages in a full cycle of oscillation ($A_x = 0.5$). Approximately symmetric isothermal contours exist near the cylinder. The cylinder motion in the in-line direction produces symmetrical perturbations which, under certain conditions, dominate over the naturally occurring antisymmetric mode of vortex shedding [21]. A high concentration of isothermal contours can be observed near the upstream and downstream stagnation points.

Transverse oscillation

The amplitude and frequency parameters of oscillation were kept the same as in the case of the in-line oscillation ($A_y = 0.25$, $A_y = 0.5$ and $F_y = 0.2$). Figure 8 shows the time dependent average Nusselt number

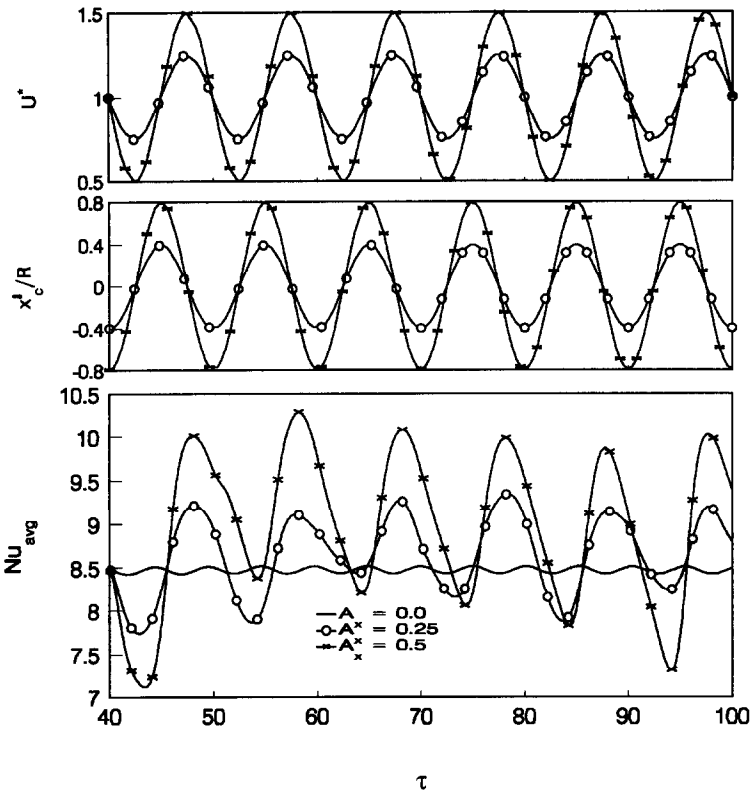

FIG. 5. Time dependent average Nusselt number (in-line oscillation).

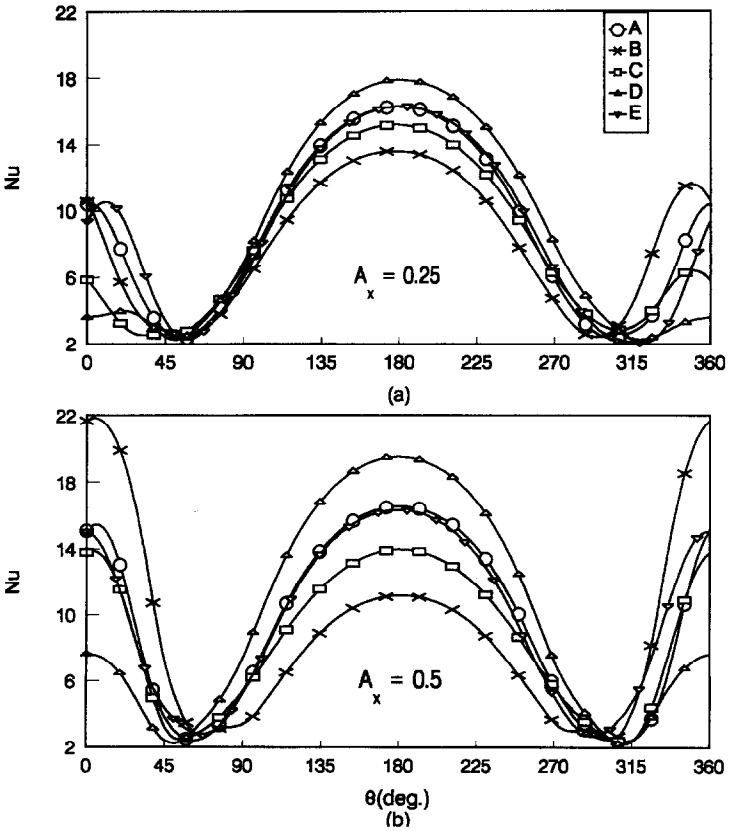

FIG. 6. Local Nusselt number distribution on the cylinder. A. $\tau^* = 0.0$, B. $\tau^* = 0.25$, C. $\tau^* = 0.5$, D. $\tau^* = 0.75$, E. $\tau^* = 1.0$.

Table 2. Location and magnitude of maximum $Nu(\theta, \tau)$ in a cycle of oscillation

	$A_y = 0.25$		$A_y = 0.5$		$A_y = 0.25$		$A_y = 0.5$	
τ^*	Max. $Nu(\theta, \tau)$	Angle (deg.)	Max. $Nu(\theta, \tau)$	Angle (deg.)	Max. $Nu(\theta, \tau)$	Angle (deg.)	Max. $Nu(\theta, \tau)$	Angle (deg.)
0.00	16.26	180	16.55	180	15.90	182.4	15.91	184.8
0.25	13.59	180	21.83	4.8	16.16	165.6	16.92	153.6
0.50	15.16	180	13.98	0, 180	15.90	177.6	15.97	175.2
0.75	17.87	180	19.53	180	16.18	196.8	16.94	206.4
1.00	16.28	180	16.33	180	15.91	182.4	15.96	184.8

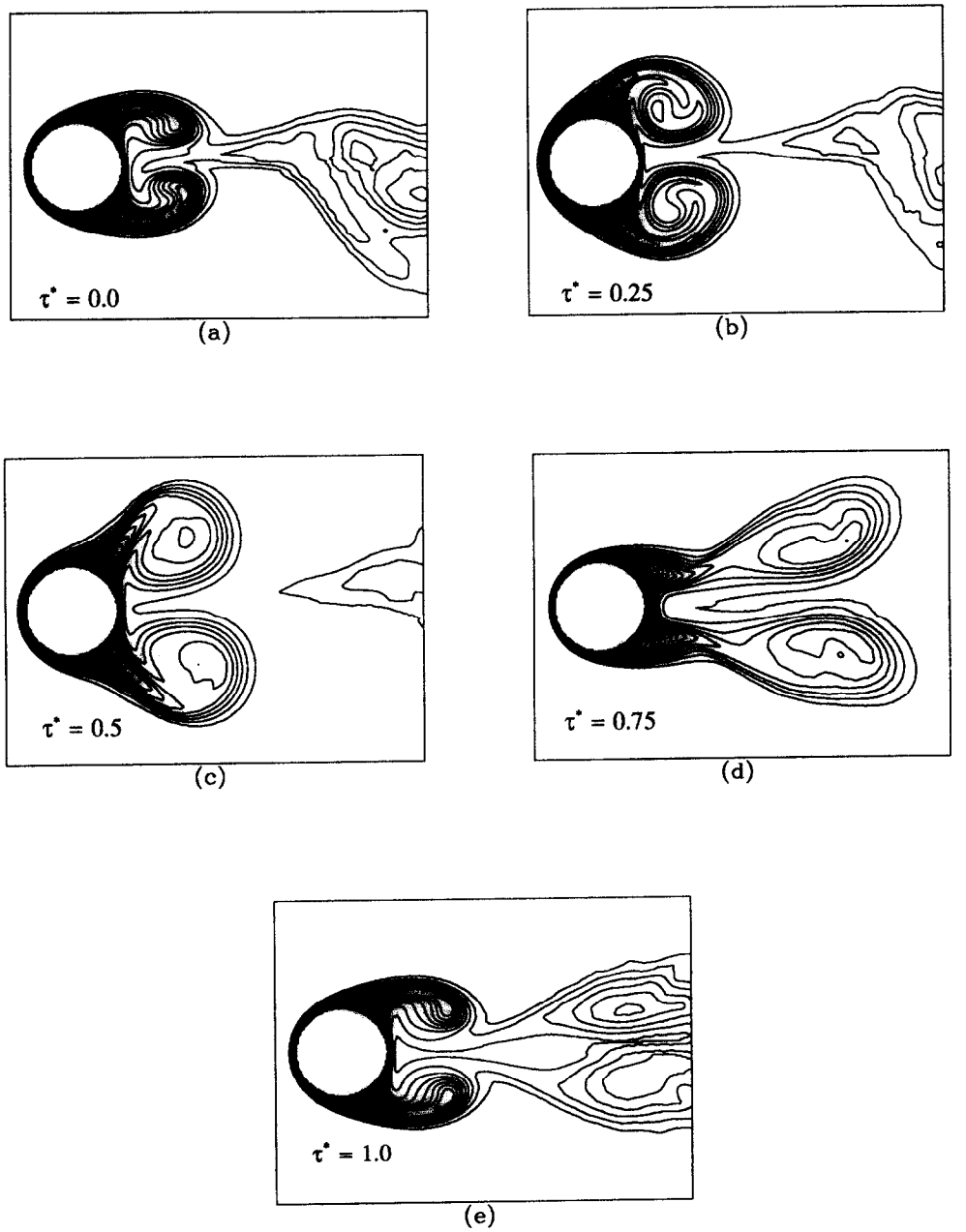

FIG. 7. Isothermal contours at various cycles of oscillation ($A_y = 0.5$). (a) Beginning of cycle; (b) after 1/4 cycle; (c) after 1/2 cycle; (d) after 3/4 cycle; (e) after one cycle.

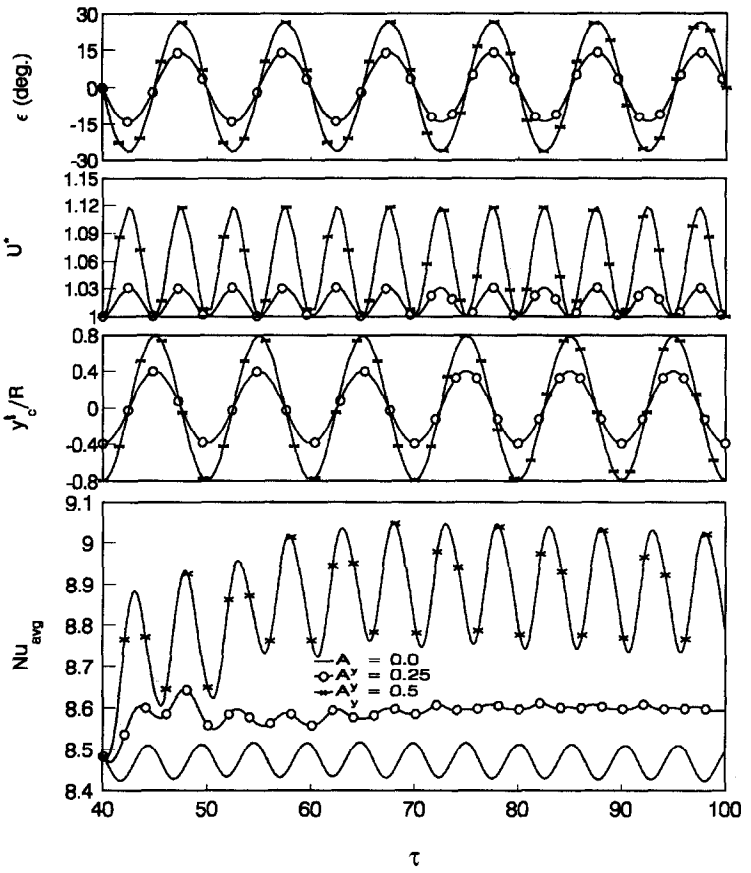

FIG. 8. Time dependent average Nusselt number (transverse oscillation).

at different velocity amplitudes in the transverse direction. The time dependent position of the cylinder in the transverse direction (y_c'/R), magnitude and incident angle of the relative free stream velocity ($|U^*| = \sqrt{\{1+A_y^2 \sin^2(\pi F_x \tau)\}}$ and ε) are also plotted above in the same figure for easy reference. Unlike in the case of in-line oscillation, $Nu_{avg}(\tau)$ oscillates at twice the frequency of oscillation of the cylinder. It is to be noticed that the magnitude of the relative free stream velocity also oscillates at $2F_y$ which directly influences the time variation of the average Nusselt number. The chosen frequency parameter lies within the lock-in frequency range. During lock-in, it is known that vortex shedding is being controlled by the cylinder oscillation. This may also influence the average Nusselt number variation with time. The mean Nusselt number increases with increasing velocity amplitude (Table 1). The computed values of Nu_m agree with the values calculated from equation (17) with a maximum difference of about 1.4%.

Figure 8 shows that amplitude of oscillation of $Nu_{avg}(\tau)$ first decreases and then increases with an increase in the velocity amplitude (A_y) in the transverse direction. This may be due to the fact that the $Nu_{avg}(\tau)$ for the case of the forced oscillation of the cylinder ($A_y = 0.5$) is approximately 180° out of phase with the naturally occurring $Nu_{avg}(\tau)$ for the stationary cylinder. As A_y increases, the effect of forced oscillation on the amplitude of $Nu_{avg}(\tau)$ becomes more predominant than that of the natural oscillation.

In any cycle of oscillation, both maximum values of $Nu_{avg}(\tau)$ occur (Fig. 8) near the zero position of the cylinder ($y_c'/R \approx 0$) during the upward and downward motion of the cylinder. The minimum values of $Nu_{avg}(\tau)$ are predicted near the minimum y_c'/R and the maximum y_c'/R. After the initial transient stage, approximately the same maximum and minimum values of $Nu_{avg}(\tau)$ occur at the same positions in every cycle.

The local heat transfer rate from the cylinder surface at velocity amplitudes 0.25 and 0.5 are represented in Figs. 9(a) and (b), respectively. The location and magnitude of maximum $Nu(\theta, \tau)$ are given in Table 2 at different times in a single cycle of oscillation of the cylinder (from $\tau = 50.0$ to 60.0). It can be observed that the location of the maximum heat transfer rate oscillates at the same frequency as that of the cylinder (F_y). The location of the maximum local Nusselt number depends on the direction of the relative velocity of the flow with respect to the cylin-

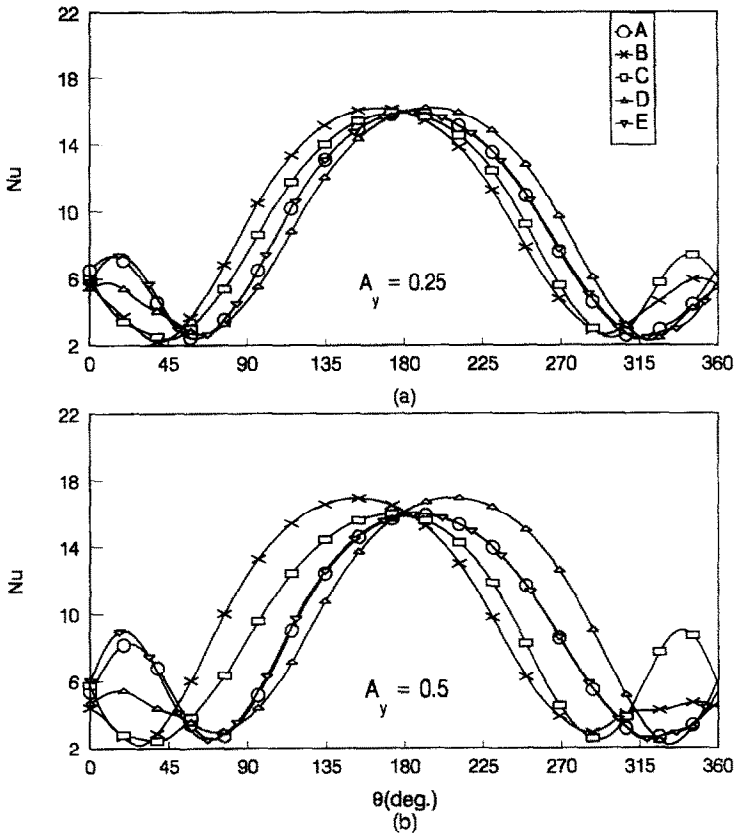

FIG. 9. Local Nusselt number distribution on the cylinder. A. $\tau^* = 0.0$, B. $\tau^* = 0.25$, C. $\tau^* = 0.5$, D. $\tau^* = 0.75$, E. $\tau^* = 1.0$.

der. This implies that the phase of the relative free stream velocity which is also oscillating at a non-dimensional frequency F_y (Fig. 8), influences directly the location of the maximum local Nusselt number on the cylinder. During the upward or downward motion of the cylinder with maximum velocity, the maximum heat transfer occurs from a location on the upper surface or the lower surface respectively. Figures 10(a)–(e) show the isothermal contour maps at different stages in single cycle of oscillation. A significant amount of difference in the layout of isothermal contours can be observed when compared with the contour maps for in-line oscillation (Figs. 7(a)–(e)). A high concentration of isothermal contours are found to exist only near the upstream stagnation point.

CONCLUSIONS

A very general formulation for forced convective heat transfer from an oscillating cylinder using vorticity and stream function as dependent variables is presented. In the case of the stationary cylinder in a cross flow, the average Nusselt number was found to be varying with a small amplitude at twice the natural shedding frequency. In comparison with the forced convective heat transfer from a stationary cylinder, an increased mean Nusselt number was predicted with the oscillation in both the in-line and the transverse directions. In the case of transverse oscillation, the average Nusselt number was found to be oscillating at twice the forced frequency of oscillation. The predicted results for the stationary cylinder and the transversely oscillating cylinder, agree satisfactorily with the values obtained from equation (17). An increasing trend of the mean Nusselt number with in-line oscillation is predicted as opposed to the decreasing trend given by the correlation. The location of maximum local Nusselt number depends on the direction and velocity amplitude of oscillation of the cylinder. The amplitude of $Nu_{avg}(\tau)$ variation is strongly influenced by the oscillating velocity amplitude.

Acknowledgement—This research work was financially supported through a University of Windsor Postgraduate Scholarship and grants from the Natural Sciences and Engineering Research Council of Canada (Grant Numbers: A-2190 and A-1403).

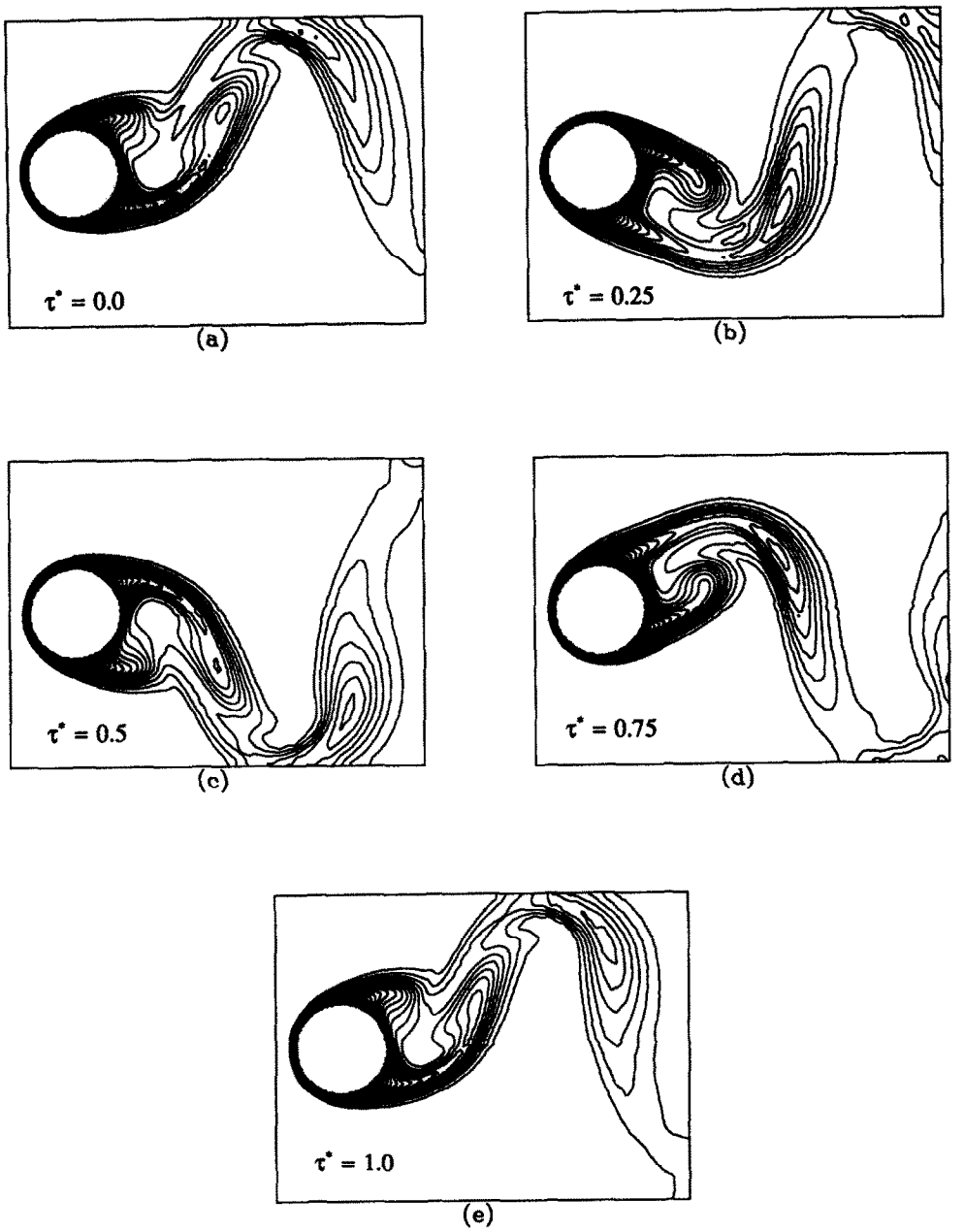

FIG. 10. Isothermal contours at various cycles of oscillation ($A_y = 0.5$). (a) Beginning of cycle; (b) after 1/4 cycle; (c) after 1/2 cycle; (d) after 3/4 cycle; (e) after one cycle.

REFERENCES

1. W. Chun and R. F. Boehm, Calculation of forced flow and heat transfer around a cylinder in cross flow, *Numer. Heat Transfer* **15**, 101–122 (1989).
2. A. S. Dawood, B. L. Manocha and S. M. J. Ali, The effect of vertical vibrations on natural convection heat transfer from a horizontal cylinder, *Int. J. Heat Mass Transfer* **24**, 491–496 (1981).
3. H. Kimoto, A. Kadotsuji and T. Hirose, Effect of vibration on the natural convection heat transfer of horizontal cylinder, *Bull. JSME* **26**(217), 1154–1161 (1983).
4. B. F. Armaly and D. H. Madsen, Heat transfer from an oscillating horizontal wire, *ASME J. Heat Transfer* **93**, 239–240 (1971).
5. J. C. Dent, The effect of acoustic and mechanical oscillation on free convection from heated cylinders in air, *Chem. Engng Sci.* **24**, 1599–1605 (1969).
6. B. G. Hegge Zijnen, Heat transfer from horizontal cylinders to a turbulent air flow, *Appl. Sci. Res.* **A7**, 205–223 (1958).
7. C. T. Leung, N. W. M. Ko and K. H. Ma, Heat transfer from a vibrating cylinder, *J. Sound Vibration* **75**(4), 581–582 (1981).

8. K. Takahashi and K. Endoh, A new correlation method for the effect of vibration on forced convection heat transfer, *J. Chem. Engng Japan* **23**(1), 45–50 (1990).
9. K. Sreenivasan and A. Ramachandran, Effect of vibration on heat transfer from a horizontal cylinder to a normal air stream, *Int. J. Heat Mass Transfer* **3**, 60–67 (1961).
10. U. C. Saxena and A. D. K. Laird, Heat transfer from a cylinder oscillating in a cross-flow, *ASME J. Heat Transfer* **100**, 684–689 (1978).
11. S. P. Kezios and K. V. Prasanna, Effect of vibration on heat transfer from a cylinder in normal flow, ASME Paper No. 66-WA/HT-43 (1966).
12. S. E. Hurlbut, M. L. Spaulding and F. M. White, Numerical solution for laminar two dimensional flow about a cylinder oscillating in a uniform stream, *ASME J. Fluids Engng* **104**, 214–222 (1982).
13. R. Chilukuri, Incompressible laminar flow past a transversely vibrating cylinder, *ASME J. Fluids Engng* **109**, 166–171 (1987).
14. K. Tsuboi, T. Tamura and K. Kuwahara, Numerical simulation of unsteady flow patterns around a vibrating cylinder, AIAA Paper No. 88-0128 (1988).
15. Y. Lecointe and J. Piquet, Flow structure in the wake of an oscillating cylinder, *ASME J. Fluids Engng* **111**, 139–148 (1989).
16. A. Borthwick, Comparison between two finite difference schemes for computing the flow around a cylinder, *Int. J. Numer. Meth. Fluids* **6**, 275–290 (1986).
17. T. P. Loc and R. Bouard, Numerical solution of the early stage of the unsteady viscous flow around a circular cylinder: a comparison with experimental visualization and measurements, *J. Fluid Mech.* **160**, 93–117 (1985).
18. J. S. Son and T. J. Hanratty, Numerical solution for the flow around a cylinder at Reynolds numbers of 40, 200 and 500, *J. Fluid Mech.* **35**(2), 369–386 (1969).
19. S. K. Jordan and J. E. Fromm, Oscillatory drag, lift and torque on a circular cylinder in a uniform flow, *Phys. Fluids* **15**(3), 371–376 (1972).
20. H. Kramers, Heat transfer from spheres to flowing media, *Physica* **12**, 61–80 (1946).
21. A. Ongoren and D. Rockwell, Flow structure from an oscillating cylinder Part 2. Mode competition in the near wake, *J. Fluid Mech.* **191**, 225–245 (1988).